JACS
JOURNAL OF THE AMERICAN CHEMICAL SOCIETY
Article
pubs.acs.org/JACS

Light-Induced Radical Formation and Isomerization of an Aromatic Thiol in Solution Followed by Time-Resolved X-ray Absorption Spectroscopy at the Sulfur K-Edge

Miguel Ochmann,[†,‡,■] Inga von Ahnen,[†,#,■] Amy A. Cordones,[§,▽] Abid Hussain,[†,‡] Jae Hyuk Lee,[§,○] Kiryong Hong,[§,∥,▼] Katrin Adamczyk,[†,‡] Oriol Vendrell,[⊥,◆] Tae Kyu Kim,[*,∥] Robert W. Schoenlein,[*,§,¶] and Nils Huse[*,†,‡]

[†]Department of Physics, University of Hamburg and Center for Free Electron Laser Science, 22761 Hamburg, Germany
[‡]Max Planck Institute for the Structure and Dynamics of Matter, 22761 Hamburg, Germany
[§]Ultrafast X-ray Science Lab, Chemical Sciences Division, Lawrence Berkeley National Laboratory, Berkeley, California 94720, United States
[∥]Department of Chemistry and Chemistry Institute of Functional Materials, Pusan National University, Busan 46241, South Korea
[⊥]Center for Free-Electron Laser Science, DESY and The Hamburg Centre for Ultrafast Imaging, 22607 Hamburg, Germany

Supporting Information

ABSTRACT: We applied time-resolved sulfur-1s absorption spectroscopy to a model aromatic thiol system as a promising method for tracking chemical reactions in solution. Sulfur-1s absorption spectroscopy allows tracking multiple sulfur species with a time resolution of ∼70 ps at synchrotron radiation facilities. Experimental transient spectra combined with high-level electronic structure theory allow identification of a radical and two thione isomers, which are generated upon illumination with 267 nm radiation. Moreover, the regioselectivity of the thione isomerization is explained by the resulting radical frontier orbitals. This work demonstrates the usefulness and potential of time-resolved sulfur-1s absorption spectroscopy for tracking multiple chemical reaction pathways and transient products of sulfur-containing molecules in solution.

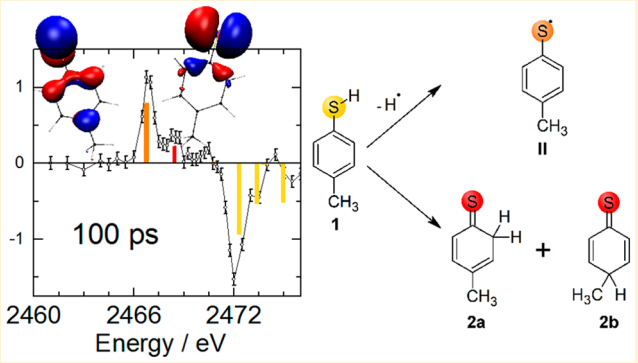

INTRODUCTION

Understanding chemical reactions on levels of atoms and electronic configurations is of major interest in most fields of chemistry, ranging from biochemistry to material sciences in order to mimic biological reactions, optimize existing chemical processes on a lab or industrial scale, or access new synthetic routes. Complex chemical reactions can be broken down into basic reaction steps, most of which involve a functional group containing one or more heteroatoms, e.g., oxygen, nitrogen, or sulfur at the reacting functional group. Sulfur is of high chemical importance as it is the tenth most abundant element in the universe and in particular, the earth's crust[1,2] and can be found in a variety of oxidation states, ranging from −2 to +6.[2,3] Its electronic versatility makes it an important element in many chemical compounds, ranging from polymers, nanoparticles, and electrode materials in batteries to molecular electronics devices. In the latter, sulfur is widely used as anchoring group for "molecular wires"[4] and in the form of thiophene-containing π-systems in organic field-effect transistors (OFETs), organic light-emitting diodes (OLEDs), and organic photovoltaics (OPVs).[5,6] Furthermore, sulfur plays an important role in biochemistry: In both peptide chains and reaction centers of proteins, sulfur is an important element, i.e., as one of the amino acids methionine (thioether) or cysteine (thiol) and as sulfide in metal−sulfur-complexes, respectively.[7]

The thiol group has a central function in many biologically important reactions such as the formation of disulfide bridges via several thiol−disulfide interchange reactions in proteins.[8−10] Thiols are also active in radical repair by donating an H atom to a radical thereby forming the more stable S-centered thiyl radical.[8,11] Thiols in general are known for their antioxidant and radical scavenging properties. The thiyl radical as the product of the repair reaction and the intermediate of thiol-including reactions in biochemistry can undergo many different secondary reactions of which some are potentially biologically harmful.[12−14] Increased protein folding and unfolding of disulfide-containing proteins by addition of substituted thiophenols in vitro has been observed as well.[10,15] Accordingly, the chemical behavior of aromatic thiols and corresponding

Received: December 22, 2016
Published: February 20, 2017

DOI: 10.1021/jacs.6b12992
J. Am. Chem. Soc. 2017, 139, 4797−4804

thiyl radicals and thiolates are of major interest for biochemical and biological applications.

Aromatic thiols show a higher nucleophilicity and reactivity toward disulfides than aliphatic thiols.[8] Photoexcitation of thiophenol and its derivatives with ultraviolet light seems to primarily result in the formation of the S-centered thiyl radicals (thiophenoxy radicals) via homolytic bond cleavage of the S−H bond.[16−18] Riyad et al. investigated the reaction kinetics of the thiophenoxy radical after photodissociation of several substituted thiophenols including 4-methylthiophenol (4-MTP, **1**) with laser flash photolysis.[18] Theory predicts the photodissociation to result from population of the repulsive $\pi\sigma^*$-state (S_2). In solution, the formation of a conical intersection between the S_2 and the ground-state S_0 would allow for direct relaxation back to the ground state, but the dissociation pathway which leads to radical formation dominates.[19−22] Accordingly, the reported decay rates of the radical population are consistent with diffusion-limited recombination. In addition, a second product was ascribed to a hydrogen adduct (H-adduct) resulting from the reaction of a hydrogen atom with the aromatic ring of the parent thiophenol molecule. A third product appearing within ∼15 μs was hypothesized to be the disulfide dimer formed by the reaction of two thiophenoxy radicals.

More recently, femtosecond ultraviolet absorption spectroscopy revealed the formation of a secondary photoproduct after photodissociation of 4-MTP on a time scale of tens of picoseconds with the same spectral footprint as the H-adduct observed by Riyad et al.,[18] which suggested the appearance of this photoproduct to coincide with the initial decay of the thiophenoxy radical.[19−21] The structure of this species was suggested to be a thione isomer, where the H atom is bound at the *ortho*-, *meta*-, or *para*-position of the phenyl ring.[21,22] Since the *meta*-adduct is thermodynamically less stable than the other products, the Bradforth group concluded that this recombination pathway is strongly disfavored.[19] However, this interpretation is tentative as the dynamical UV and vibrational studies are based in part on theoretical predictions with only qualitative agreement with experiment. A clear spectral identification of the transient photoproducts is paramount for a reliable understanding of the reaction mechanism. Unfortunately, optical probes are generally very difficult to simulate quantitatively, even with high-level electronic structure calculations, due to strong electron−electron correlations and the broad and often nondescript nature of valence-to-valence transitions.

In this work we investigate the photochemistry of 4-MTP (**1**) with time-resolved X-ray absorption spectroscopy (TRXAS) at the sulfur K-edge, which is capable of following reaction dynamics of sulfur-containing systems with elemental specificity. The abundant body of literature on studies employing static sulfur K-edge XAS to molecular systems both experimentally and theoretically[23−40] underscores the usefulness and important information content of sulfur-1s spectroscopy. Pairing the high chemical specificity of spectroscopy in the soft,[41−44] tender,[45−48] and hard[49−55] X-ray range with time-resolved methods is becoming an established spectroscopic tool for structural dynamics by tracking the relevant atomic species during ultrafast chemical reactions. TRXAS exploits the inherent element specificity of core-level transitions, the initial state of which is highly localized and of well-defined symmetry and spin. Moreover, distinct spectral features of atomic species in different oxidation and spin states permit the precise assignment of photoproducts, thereby allowing TRXAS to follow dynamics of electronic and molecular structure more precisely than valence spectroscopy permits. The sensitivity of X-ray absorption spectra to bond order, symmetry, and valence charge distribution around the absorbing atomic species can be particularly useful in the identification of different reaction intermediates and products when multiple reaction pathways are present. In particular, sulfur-1s absorption spectroscopy is known to exhibit large spectral separations for different chemical environments of the sulfur atom.[56−61] It permits identifying the chemical state of sulfur-containing functional groups very precisely and with atomic resolution for spectrally distinct sulfur sites within a molecule or among different photoproducts. In the following, we present a time-resolved study at the sulfur K-edge with sulfur 1s → 3p transitions as a probe of molecular dynamics of 4-MTP in cyclohexane solution.

METHODS

Experimental Setup. All experiments were conducted at beamline 6.0.1. of the Advanced Light Source in Berkeley, California, and the experimental setup has been described previously.[62,63] The experimental setup is shown in Figure 1. The filling pattern of the storage ring consists of 276 electron bunches, one of which is placed in a 100 ns gap for isolated detection. A 4-kHz heat-load chopper transmits 10-μs long X-ray bunch trains. The X-ray beam is monochromatized with a cryogenically cooled Si(111) double-crystal monochromator ($\Delta E/E$ = 1/7000). The X-ray pulses are focused to 170 μm × 250 μm at the sample position.

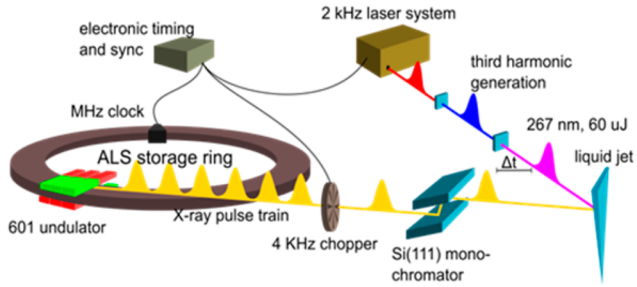

Figure 1. Schematic drawing of the experimental setup at beamline 6.0.1 of the Advanced Light Source.

Pump pulses at 267 nm from a third harmonic generator (THG) of the Ti:sapphire 800 nm pulses are focused with a CaF_2 lens to 270 μm × 300 μm with 60 μJ at the sample position, impinging on the liquid jet at an angle of 15° with respect to the X-ray pulses. The laser oscillator is locked to the subharmonic of the 500 MHz radio frequency (RF) clock of the synchrotron storage ring while the Pockels cells of the laser amplifier are triggered by the X-ray chopper. Timing between X-rays and laser pulses is controlled by a phase shifter between the laser oscillator and the RF clock.

Static absorption spectra were collected in total fluorescence yield (TFY) using an integrating photodiode and a current amplifier. Transient differential absorption spectra are recorded in transmission at 4 kHz while the sample is intermittently excited at 2 kHz. The X-ray probe pulses impinged on an avalanche photodiode (APD) which is shielded from laser radiation with 200 nm of aluminum foil. The APD signal is amplified and sent to a boxcar integrator. The sample is delivered through a 100-μm wide sapphire nozzle by a gear pump at flow rates of >0.5 mL/s. Prior to data collection, the sample chamber was evacuated and filled with helium to 1 atm.

Chemicals and Materials. 4-MTP and cyclohexane were purchased from Sigma-Aldrich, and used without further purification. Cyclohexane solutions of 4-MTP (200 mM) were prepared by

DOI: 10.1021/jacs.6b12992
J. Am. Chem. Soc. 2017, 139, 4797−4804

dissolving 12.4 g of 4-MTP in 500 mL of cyclohexane. Samples were always replaced after 8 h of use.

Theoretical Calculations. The equilibrium geometries of all molecular species were obtained by second order Møller–Plesset perturbation theory[64] (MP2) with the Dunning correlation consistent basis set aug-cc-pvtz[65] using the Gaussian 09 program package.[66] In order to simulate the X-ray absorption spectra, the first-principles multireference restricted active space self-consistent field (RASSCF) method was used with no symmetry imposed. The active space for simulated XAS comprised 14 electrons distributed over 13 orbitals. The aug-cc-pvtz basis is used for sulfur and the three adjacent carbon atoms, while aug-cc-pvdz was used on all other atomic centers. The energies of the computed states were further improved by applying second order perturbation theory (RASPT2)[67−69] to RASSCF wave functions to account for dynamic correlation effects. In the RASSCF calculations of core-excited states, the core orbital was kept in the RAS3-subspace, thus restricting the possible configurations to those with at least one electron missing from the core orbital and preventing a variational collapse during the wave function optimization that would refill the core-hole with a valence electron (this sorting of electrons into active spaces is known as the core-RAS method).[70] RASSCF/RASSI calculations were performed with the Molcas 7.8 program suite.[71] All transition energies were rescaled by a constant factor (equating to an energy shift of about −2.8 eV) such that the computed 4-MTP spectrum matches the experimental one.

RESULTS AND DISCUSSION

Figure 2A shows the static X-ray absorption spectrum of 4-MTP in cyclohexane at the sulfur K-edge. Two prominent transitions are observed at 2472.5 and 2473.6 eV, along with additional less resolved transitions above 2475 eV which merge into the actual continuum edge. The resulting differential absorption spectrum upon ultraviolet excitation at 267 nm (4.64 eV) at a pump–probe time delay of 100 ps is shown in Figure 2B. The negative bleaching signal at 2472.5 eV signals a loss of absorption and coincides with the two main absorption peaks of the ground state. Three induced absorption features emerge at energies of 2467.0, 2468.5, and 2470.3 eV, respectively. The apparent area ratio of the energetically lowest two peaks is about 1:3 while the small induced absorption is hard to quantify and only appears at high excitation fluence (see discussion below). Pump–probe transients at photon energies of the strongest absorption changes fully emerge within the time resolution of our experiment (~70 ps) and stay constant over the observed time frame of about 500 ps, as does the ground-state bleaching signal. For details on the experimental time traces and their modeling see the Supporting Information.

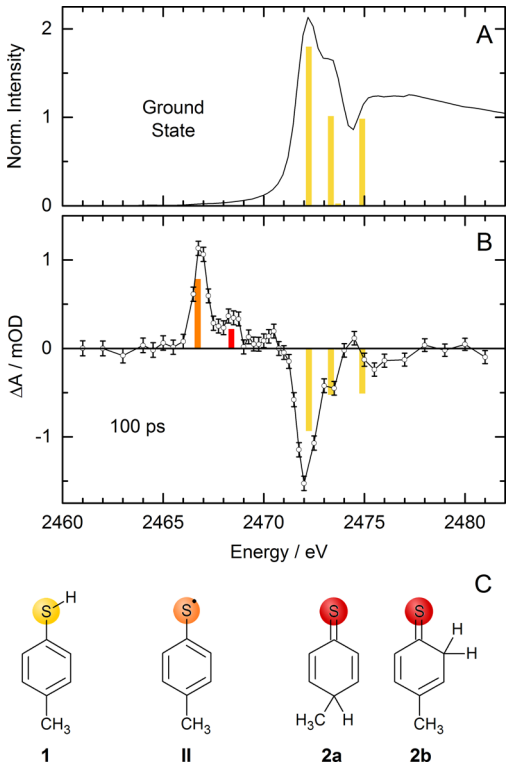

Figure 2. (A) Static sulfur-1s absorption spectrum of 4-MTP in cyclohexane solution and calculated lowest S-1s transitions (yellow). (B) Differential absorption spectrum at 100 ps after 267 nm excitation (50 mJ/cm^2), and calculated S-1s transitions for ground-state bleach and observed photoproducts: 4-MTP (yellow), radical (orange), and thione isomers (red). (C) Structures of 4-MTP (**1**), 4-methylthiophenoxy radical (**II**), and *ortho*- (**2a**) and *para*- (**2b**) thiones.

In order to identify the spectra in Figure 2, we employed RASSCF calculations to predict the sulfur-1s transitions of the ground state of 4-MTP (**1**) and possible photoproducts in order to recreate the experimental differential spectrum at 100 ps. Figure 2A shows three distinct transitions that match the experimentally observed ground-state transitions around 2472 eV very well. We have not convolved the transition lines with a Voigt profile for clarity. However, a monochromator resolution of σ = 0.35 eV and a Lorentzian lifetime broadening of 0.8 eV reproduce the main absorption features in Figure 2A (for convolved data see Figure S2). We note that our high-level electronic structure calculations neither describe the Rydberg series nor the atomic continuum absorption edge. Other theoretical approaches would be more appropriate for describing multiple scattering and the EXAFS region. However, RASSCF provides a very accurate approach to describing electronic correlations, and the bound–bound transitions relevant to this experimental study.

The initial chemical reaction step in 4-MTP upon excitation with 267 nm pulses is the cleavage of the S–H bond. Oliver et al. reasoned for homolytic bond dissociation with production of a hydrogen atom, a 4-methylthiophenoxy radical, and an additional adduct.[19] The 4-methylthiophenoxy radical (**II**) as shown in Figure 2C exhibits a theoretical S-1s spectrum that matches the experimentally observed induced absorption peak at 2467 eV, underscoring that indeed photoinduced homolytic bond cleavage occurs. However, the methylthiophenoxy radical alone does not reproduce our experimentally observed differential absorption spectrum at 100 ps. Another induced absorption peak at 2468.5 eV is clearly discernible.

In order to identify this feature, we have computed spectra for two 4-methylthiophenoxy ions, as these are most closely related to the 4-methylthiophenoxy radical (**II**): the formally hydride-abstracted cation (**Ia**) and the thiolate anion (**III**), both of which could be produced through heterolytic S–H bond dissociation. However, the computed sulfur-1s transitions of the cations (**Ia** and **Ib**) and the thiolate anion (**III**) deviate notably from the experimentally observed spectral feature at 2468.5 eV (see Figure S3). Moreover, the ejection of a hydride anion seems very unlikely since sulfur is the more electronegative atom in the S–H bond, polarizing the bond toward the sulfur atom. Two-photon ionization of 4-MTP toward the cation (**Ib**) at 9.3 eV seems possible[72] albeit the first ionization energy of elementary sulfur is at 10.36 eV.[73]

DOI: 10.1021/jacs.6b12992
J. Am. Chem. Soc. 2017, 139, 4797–4804

Instead, we consider the three possible thione isomers to explain the observed emergence of this new spectral feature. These species can emerge when the photolytically cleaved hydrogen atom attaches to the aromatic ring of the parent 4-MTP radical residue, either in the *ortho-* (**2a**), *para-* (**2b**), or *meta-* (**2c**) position (see also Scheme S1), thereby disrupting the π-conjugation of the ring. The corresponding calculated lowest sulfur-1s transitions for **2a** and **2b**, namely, 4-methylcyclohexa-2,4-diene-1-thione (**2a**) and 4-methylcyclohexa-2,5-diene-1-thione (**2b**), henceforth denoted as *ortho-* (**2a**) and *para-* (**2b**) thione, respectively, both match the second observed induced absorption peak at 2468.5 eV very well. The dominant transition of the *ortho*-thione is predicted 0.15 eV lower in spectral position and with 20% higher amplitude than the *para*-thione. A distinction between the two isomers with sulfur-1s absorption spectroscopy is difficult due to the inherent lifetime broadening of ~0.8 eV. The *ortho*-thione assignment matches slightly better with the experimental data.

The nearly identical transition energies of both thione isomers point to the fact that the S-1s transitions are strongly influenced by the bonding order and oxidation state of the sulfur atom. For both thione isomers, the dominating feature is the C═S double bond. The position of the newly formed sp^3-hybridized carbon does not influence the electronic structure of the sulfur atom substantially because the sulfur atom and the newly formed CH_2 (**2a**) or $CHCH_3$ (**2b**) group are separated by either two (**2a**) or four (**2b**) chemical bonds, respectively. The *meta*-adduct **2c** cannot be described as a stable thione product in the conventional Lewis formalism but has to be conceived as a delocalized biradical which manifests itself as an energetically highly disfavored species[19] with sulfur-1s transitions appearing at much higher energy than the induced absorption peak at 2468.5 eV in Figure 2B (see also Scheme S1). Recently, Reva et al. found clear evidence for the formation of the thione isomers **2a** and **2b** upon photoexcitation. Steady-state infrared spectroscopy was used in cryogenic argon matrices in which these isomers form extremely long-lived metastable states.[74] Moreover, no evidence for the formation of the *meta*-adduct **2c** was found while photoexcitation with 267 nm light resulted in the formation of **2a** and **2b**. These results are in excellent agreement with our findings. However, our method observes the photochemistry of 4-MTP under ambient conditions in real time, i.e., in the liquid phase at room temperature, with a site-specific electronic- and structural-probe.

Our theoretical calculations provide detailed information on the electronic structure of the different sulfur species. In the following, we discuss the character of the spectral lines in terms of highest occupied and lowest unoccupied molecular orbitals (HOMOs and LUMOs, respectively), as well as the singly occupied molecular orbital (SOMO) for the 4-MTP radical. In the ground state of 4-MTP, we observe three major transitions as observed in Figure 2A. The lowest sulfur-1s transition is predominantly (>90%) described by the population of the LUMO + 2 orbital as shown in Figure 3. The two higher-lying transitions in Figure 2A are well-described by linear combinations of LUMO + 3 ± LUMO + 5 with less than 10% from other states. For the 4-MTP radical (**II**) and the thione isomers **2a** and **2b**, only one major transition in each species is found. These transitions are dominated by a single configuration, populating the LUMO (thione) and the SOMO (radical), respectively (Figure 3). Additional transitions are

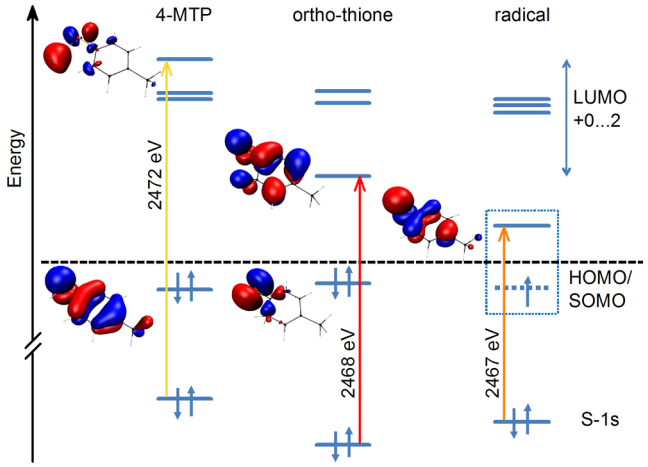

Figure 3. Molecular orbitals and corresponding isosurfaces relevant to the lowest sulfur-1s transitions in the three main species (4-MTP (**1**), *ortho*-thione (**2a**), 4-MTP radical (**II**)).

smaller by at least 2 orders of magnitude compared to the respective major transitions depicted in Figure 2. From the orbital scheme in Figure 3, the relative shift of the lowest absorptive sulfur-1s transitions in Figure 2B can be inferred qualitatively for each species: The HOMO−LUMO gap follows a clear trend that reflects the relative energetic stability of the three sulfur species. The relative energy difference between the sulfur-1s orbital and the dominating orbital of the sulfur-1s excitations decreases in the same order from 4-MTP (1s → LUMO + 2) via the thione (1s → LUMO + 0) to the radical (1s → β-SOMO). In the radical, the energy level scheme exhibits additional complexity because the unpaired electron divides the transitions into α- and β-densities, owing to the fact that transition energies of spin-up and spin-down excitations interact differently with the unpaired electron of the SOMO. The calculations are also able to explain the regioselectivity of the observed thione isomerization: In the 4-MTP radical (**II**), the HOMO is a SOMO, which governs the radical's chemistry. As can be seen from the isosurface for the SOMO in Figure 3, even though the radical is mainly sulfur-centered, there is also electron density at the *ortho-* and *para*-carbon atoms and none at the *meta*-carbon atoms. This is a manifestation of the regioselectivity of the observed thione isomerization reaction which strongly disfavors the *meta*-form.

It is also instructive to consider the trend of the sulfur-1s orbital energies for **1**, **II**, and **2a**: Recent publications provide evidence that the 1s-orbital energies in transition-metal complexes are strongly correlated with the amount of effective valence charge on a bound nitrogen atom.[44,75,76] The N-1s spectra were found to be similarly correlated because they depended mainly on the N-1s orbital energy in these compounds. We performed a natural population analysis to check for a similar correlation between valence charge and S-1s orbital energy. The results are given in Table 1 along with the calculated sulfur−carbon bond distance. There is a significant

Table 1. Bond Distance and Natural Populations

	4-MTP	thione	radical
d(C−S)/Å	1.77	1.64	1.73
nat pop	0.042	−0.043	0.056[a]

[a]Natural populations of α and β spin densities were added.

DOI: 10.1021/jacs.6b12992
J. Am. Chem. Soc. 2017, 139, 4797−4804

Scheme 1. Reaction Pathways of 4-MTP upon 267 nm Excitation

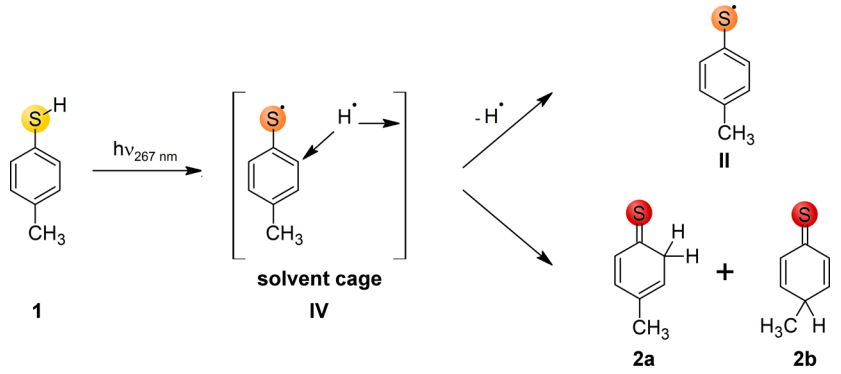

bond contraction (>10 pm) between the sulfur and carbon atom upon transition from the ground-state 4-MTP molecule to the thione isomers **2a** or **2b** as expected for a double bond formation. This change is accompanied by a significant reduction in the natural population of the sulfur atom, leading to a lower S-1s orbital energy and signaling a reduced valence charge density on the sulfur atom. The sulfur radical does not reveal significant differences from the 4-MTP parent compound. We interpret this finding as a manifestation of the relative inertness and stability of sulfur radicals compared to the very reactive oxygen radicals. X-ray photoemission spectroscopy is sensitive to these binding energies while transition energies of X-ray absorption spectra depend not only on the binding energy of the core-level electrons but also on the dipole selection rules dictated by the symmetries of the respective LUMO states. This fact can lead to a seeming lack of systematic ordering of transitions while the basic concept of core−electron screening by an atom's valence charge density still holds.

The differential spectrum in Figure 2B exhibits a third induced absorption peak at 2470.3 eV which appears only at high pump fluence of 50 mJ/cm^2 while it is absent at half the fluence (Figure S4). We have considered several possible species (Scheme S1) for this induced absorption peak of which the calculated 4-MTP anion (**III**) absorption best matches the observed spectral position (Figure S3). We cannot exclude that the anion species could emerge from highly excited states upon multiphoton absorption. However, it is known that cyclic aliphatic hydrocarbons undergo multiphoton absorption in strong femtosecond laser fields, producing fast decaying hydrocarbocations and free solvated electrons.[77] Such electrons constitute a highly reactive species and could react via a single electron transfer (SET) process with a 4-MTP radical (**II**) to yield the 4-MTP anion (**III**) within our time resolution. A second species with nearby sulfur-1s transitions is the 4-MTP dimer, the generation of which can result from two 4-MTP radicals (**II**). This diffusion-limited process cannot occur in the measured time frame (<1 ns) although Riyad et al. observed a product formation on microsecond time scales which they interpreted as dimerization. Only the formation of prearranged dimers, trimers, and tetramers of aromatic thiols would allow for dimerization to occur rapidly enough. Oligomers of aromatic thiols have been reported in solution, where the thiol group of one molecule coordinates to the π-system of another molecule. It is possible that such dimer formation occurs under our experimental conditions of 200 mM 4-MTP concentration. However, the 4-MTP dimer has its lowest absorption peak above 2471 eV. We therefore exclude dimerization and attribute the fluence-dependent induced absorption to anion formation.

We end the discussion with a few considerations of the temporal evolution of the 4-MTP photochemistry. The observed initial photofragmentation of 4-MTP into 4-MTP radicals (**II**) and hydrogen atoms occurs on an ultrafast time scale which eludes our time resolution of ∼70 ps, and for the initial reaction dynamics, we refer to Zhang et al.[20] Upon UV excitation the 4-MTP molecule is photodissociated to generate a radical pair **IV** in Scheme 1. The excess excitation energy is converted to kinetic energy and carried largely by the hydrogen atom, which is ejected into the solvent shell with an average ejection length of 9 Å or about two to three solvent spheres.[20] Suppression of fast geminate S−H recombination at such large ejection lengths is characteristic of weak solute−solvent interaction as found in cyclohexane solution. The initial radical concentration was observed to partially decay to a constant value within less than 50 ps.[20] The H-adduct, which we identify as the thione isomers **2a** and **2b**, emerges at the same rate.[20] No change in the relative populations occurs in the observed subnanosecond time frame, in agreement with the time evolution of the signal (Figure S1).

The reaction pathways are depicted in Scheme 1: Upon photoexcitation, 4-MTP (**1**) is promoted to a dissociative state, and the hydrogen atom is ejected into the surrounding solvent cage (**IV** in Scheme 1). The H atom will either escape the solvation shell, producing the long-lived 4-methylthiophenoxy radical (**II**), or attach to the aromatic ring of the parent 4-MTP molecule yielding the thione isomers **2a** and **2b**. If the 4-MTP radical (**II**) survives, it will only be consumed upon diffusion-limited recombination with a hydrogen atom or another 4-MTP radical (**II**). Solvent hydrogen abstraction seems less likely given the long radical lifetime extracted from flash-photolysis studies.[18] Matrix isolation studies[74] have demonstrated optical switching between the thione isomers **2a** and **2b**, but it is unclear whether these two isomers will form both or interconvert at room temperature in solution. Time-resolved vibrational exchange spectroscopy could provide an answer because the isomers have discernible infrared spectral fingerprints.[74] Lastly, we note that in the same matrix isolation studies UV excitation of thione adducts has resulted in reformation of the 4-MTP ground state. This observation explains the low quantum yield of radical formation in nanosecond flash-photolysis studies: Thione formation occurs within a few picoseconds, and a nanosecond UV excitation pulse will therefore partly consume the thione isomers and generate the 4-MTP parent species again.

DOI: 10.1021/jacs.6b12992
J. Am. Chem. Soc. 2017, 139, 4797−4804

CONCLUSIONS AND OUTLOOK

We have successfully followed a chemical reaction in the liquid phase using sulfur-1s absorption spectroscopy to reveal the different reaction pathways of an aromatic thiol model system (4-MTP) following irradiation with 267 nm light, namely radical generation, thione isomerization, and anion formation. High-level theoretical calculations permit assigning the two prominent spectral signatures to the 4-MTP radical and the thione isomers. The regioselectivity of the isomerization reaction is governed by the radical SOMO which only has high electron density on the sulfur and the *ortho*- and *para*-carbon atoms, favoring S−H recombination or isomerization to the observed *ortho*- and *para*-thiones.

Time-resolved sulfur-1s spectroscopy provides new insight beyond the corresponding optical spectroscopy techniques: It is element specific and well-described by theory. The high spectral sensitivity to different oxidation states and chemical surroundings of the sulfur atom renders this technique a valuable tool to study chemical reactions involving sulfur functional groups. Sulfur-1s spectroscopy can be applied to various systems, both in solution and in solids, and could be especially useful in the field of battery research and X-ray radiation damage of proteins (in operando, in crystallo). In combination with free-electron lasers or laser-plasma sources, sulfur-1s spectroscopy can follow chemical reactions of sulfur functional groups on atomic and possibly electronic time scales due to ultrashort and bright femtosecond X-ray pulses. This would allow for the observation of initial reaction steps and help disentangle the emergence of different photoproducts and their potential conversion of one initially formed photoproduct into another. In summary, our study underscores the potentially broad applicability of time-resolved sulfur-1s spectroscopy to follow the evolution of sulfur atoms in a variety of different bonding situations and oxidation states making it a valuable tool to study chemical reactions of sulfur-containing functional groups and materials.

ASSOCIATED CONTENT

Supporting Information

The Supporting Information is available free of charge on the ACS Publications website at DOI: 10.1021/jacs.6b12992.

Overview over all described species, and calculated sulfur 1s-spectra of all described species (PDF)

AUTHOR INFORMATION

Corresponding Authors

*tkkim@pusan.ac.kr
*rwschoen@slac.stanford.edu
*nils.huse@uni-hamburg.de

ORCID

Oriol Vendrell: 0000-0003-4629-414X
Tae Kyu Kim: 0000-0002-9578-5722
Nils Huse: 0000-0002-3281-7600

Present Addresses

[#]I.v.A.: Division of Solid State Physics, NanoLund, Lund University, Lund 221 00, Sweden.
[▽]A.A.C.: PULSE Institute, SLAC National Accelerator Laboratory, Menlo Park, CA 94025, United States.
[○]J.H.L.: Pohang Accelerator Laboratory, San-31 Hyoja-dong Pohang, Kyungbuk 790-784, South Korea.
[▼]K.H.: Center for Gas Analysis, Division of Metrology for Quality of Life, Korea Research Institute of Standards and Science, Daejeon 34113, Republic of Korea.
[◆]O.V.: Department of Physics and Astronomy, Aarhus University, 8000 Aarhus, Denmark.
[¶]R.W.S.: Linac Coherent Light Source, SLAC National Accelerator Laboratory, Menlo Park, CA 94025, United States.

Author Contributions

[■]M.O. and I.v.A. contributed equally.

Notes

The authors declare no competing financial interest.

ACKNOWLEDGMENTS

This work was supported by the Director, Office of Science, Office of Basic Energy Sciences, the Chemical Sciences, Geosciences, and Biosciences Division under the Department of Energy, Contract No. DE-AC02-05CH11231 (A.A.C., K.H., J.H.L., and R.W.S.). This research was supported by Basic Science Research Program (2013S1A2A2035406, 2014R1A4A1001690 and 2016R1E1A1A01941978) and in part by the Max Planck POSTECH/KOREA Research Initiative Program (2016K1A4A4A01922028) through the National Research Foundation of Korea (NRF) funded by Ministry of Science, ICT & Future Planning (T.K.K. and K.H.). M.O., I.v.A., K.A., and N.H. acknowledge funding from the Max Planck Society and the City of Hamburg. M.O. and N.H. gratefully acknowledge financial support of this work through the Deutsche Forschungsgemeinschaft within the Sonderforschungsbereich 925 "Light induced dynamics and control of correlated quantum systems". This research used resources of the Advanced Light Source (LBNL), which is a DOE Office of Science User Facility. The authors would like to thank Bruce Rude for his continuous support of the experimental hardware.

REFERENCES

(1) Alpher, R. A.; Herman, R. C. *Rev. Mod. Phys.* **1950**, *22*, 153.
(2) 15—Sulfur. In *Chemistry of the Elements*, 2nd ed.; Greenwood, N.N., Earnshaw, A., Eds., Butterworth-Heinemann: Oxford, 1997; pp 645 − 746.
(3) Vairavamurthy, A. *Spectrochim. Acta, Part A* **1998**, *54* (12), 2009−2017.
(4) Reed, M. A.; Zhou, C.; Muller, C. J.; Burgin, T. P.; Tour, J. M. *Science* **1997**, *278* (5336), 252−254.
(5) Meng, L.; Fujikawa, T.; Kuwayama, M.; Segawa, Y.; Itami, K. *J. Am. Chem. Soc.* **2016**, *138* (32), 10351−10355.
(6) Johnson, A. S.; Miseikis, L.; Wood, D. A.; Austin, D. R.; Brahms, C.; Jarosch, S.; Strüber, C. S.; Ye, P.; Marangos, J. P. *Struct. Dyn.* **2016**, *3*, 062603.
(7) Dey, A.; Chow, M.; Taniguchi, K.; Lugo-Mas, P.; Davin, S.; Maeda, M.; Kovacs, J. A.; Odaka, M.; Hodgson, K. O.; Hedman, B.; Solomon, E. I. *J. Am. Chem. Soc.* **2006**, *128*, 533−541.
(8) Schoeneich, C. *Methods Enzymol.* **1995**, *251*, 45.
(9) Mamathambika, B. S.; Bardwell, J. C. *Annu. Rev. Cell Dev. Biol.* **2008**, *24* (1), 211−235.
(10) DeCollo, T. V.; Lees, W. J. *J. Org. Chem.* **2001**, *66* (12), 4244−4249.
(11) von Sonntag, C.; Schuchmann, H.-P. *Methods Enzymol.* **1994**, *233*, 47.
(12) Schoeneich, C.; Dillinger, U.; von Bruchhausen, F.; Asmus, K.-D. *Arch. Biochem. Biophys.* **1992**, *292* (2), 456−467.
(13) Deneke, S. M *Curr. Top. Cell. Regul.* **2001**, *36*, 151−180.
(14) Asmus, K.-D. *Methods Enzymol.* **1990**, *186*, 168−180.
(15) Gough, J. D.; Gargano, J. M.; Donofrio, A. E.; Lees, W. J. *Biochemistry* **2003**, *42* (40), 11787−11797.
(16) Thyrion, F. C. *J. Phys. Chem.* **1973**, *77* (12), 1478−1482.

DOI: 10.1021/jacs.6b12992
J. Am. Chem. Soc. 2017, 139, 4797−4804

(17) Nakamura, M.; Ito, O.; Matsuda, M. *J. Am. Chem. Soc.* **1980**, *102* (2), 698−701.
(18) Riyad, Y. M.; Naumov, S.; Hermann, R.; Brede, O. *Phys. Chem. Chem. Phys.* **2006**, *8* (14), 1697.
(19) Oliver, T. A. A.; Zhang, Y.; Ashfold, M. N. R.; Bradforth, S. E. *Faraday Discuss.* **2011**, *150*, 439−458.
(20) Zhang, Y. Y.; Oliver, T. A. A.; Ashfold, M. N. R.; Bradforth, S. E. *Faraday Discuss.* **2012**, *157*, 141−163.
(21) Zhang, Y.; Oliver, T. A. A.; Das, S.; Roy, A.; Ashfold, M. N. R.; Bradforth, S. E. *J. Phys. Chem. A* **2013**, *117* (46), 12125−12137.
(22) Murdock, D.; Harris, S. J.; Karsili, T. N. V.; Greetham, G. M.; Clark, I. P.; Towrie, M.; Orr-Ewing, A. J.; Ashfold, M. N. R. *J. Phys. Chem. Lett.* **2012**, *3* (24), 3715−3720.
(23) Smith, T. A.; Dewitt, J. G.; Hedman, B.; Hodgson, K. O. *J. Am. Chem. Soc.* **1994**, *116* (9), 3836−3847.
(24) Evans, J.; Corker, J. M.; Hayter, C. E.; Oldman, R. J.; Williams, B. P. *Chem. Commun.* **1996**, *12*, 1431−1432.
(25) Glaser, T.; Hedman, B.; Hodgson, K. O.; Solomon, E. I. *Acc. Chem. Res.* **2000**, *33* (12), 859−868.
(26) Szilagyi, R. K.; Bryngelson, P. A.; Maroney, M. J.; Hedman, B.; Hodgson, K. O.; Solomon, E. I. *J. Am. Chem. Soc.* **2004**, *126* (10), 3018−3019.
(27) Dey, A.; Glaser, T.; Moura, J. J. G.; Holm, R. H.; Hedman, B.; Hodgson, K. O.; Solomon, E. I. *J. Am. Chem. Soc.* **2004**, *126* (51), 16868−16878.
(28) Dey, A.; Okamura, T.; Ueyama, N.; Hedman, B.; Hodgson, K. O.; Solomon, E. I. *J. Am. Chem. Soc.* **2005**, *127* (34), 12046−12053.
(29) Dey, A.; Chow, M.; Taniguchi, K.; Lugo-Mas, P.; Davin, S.; Maeda, M.; Kovacs, J. A.; Odaka, M.; Hodgson, K. O.; Hedman, B.; Solomon, E. I. *J. Am. Chem. Soc.* **2006**, *128* (2), 533−541.
(30) Dey, A., Jr.; Jenney, F. E.; Francis, E.; Adams, M. W. W.; Johnson, M. K.; Hodgson, K. O.; Hedman, B.; Solomon, E. I. *J. Am. Chem. Soc.* **2007**, *129* (41), 12418−12431.
(31) Dey, A.; Jiang, Y.; Ortiz de Montellano, P.; Hodgson, K. O.; Hedman, B.; Solomon, E. I. *J. Am. Chem. Soc.* **2009**, *131* (22), 7869−7878.
(32) Sarangi, R.; Frank, P.; Benfatto, M.; Morante, S.; Minicozzi, V.; Hedman, B.; Hodgson, K. O. *J. Chem. Phys.* **2012**, *137* (20), 205103.
(33) Hackett, M. J.; Smith, S. E.; Paterson, P. G.; Nichol, H.; Pickering, I. J.; George, G. N. *ACS Chem. Neurosci.* **2012**, *3* (3), 178−185.
(34) Pin, S.; Huthwelker, T.; Brown, M. A.; Vogel, F. *J. Phys. Chem. A* **2013**, *117* (35), 8368−8376.
(35) Koenig, C. F. J.; Schuh, P.; Huthwelker, T.; Smolentsev, G.; Schildhauer, T. J.; Nachtegaal, M. *Catal. Today* **2014**, *229*, 56−63.
(36) Donahue, C. M.; Lezama Pacheco, J. S.; Keith, J. M.; Daly, S. R. *Dalton Trans.* **2014**, *43* (24), 9189−9201.
(37) Ha, Y.; Tenderholt, A. L.; Holm, R. H.; Hedman, B.; Hodgson, K. O.; Solomon, E. I. *J. Am. Chem. Soc.* **2014**, *136* (25), 9094−9105.
(38) Pascal, T. A.; Pemmaraju, C. D.; Prendergast, D. *Phys. Chem. Chem. Phys.* **2015**, *17* (12), 7743−7753.
(39) Wujcik, K. H.; Pascal, T. A.; Pemmaraju, C. D.; Devaux, D.; Stolte, W. C.; Balsara, N. P.; Prendergast, D. *Adv. Energy Mater.* **2015**, *5* (16), 1500285.
(40) Martin-Diaconescu, V.; Kennepohl, P. *J. Am. Chem. Soc.* **2007**, *129* (11), 3034−3035.
(41) Wen, H.; Huse, N.; Schoenlein, R. W.; Lindenberg, A. M. *J. Chem. Phys.* **2009**, *131*, 234505.
(42) Wernet, Ph.; Kunnus, K.; Josefsson, I.; Rajkovic, I.; Quevedo, W.; Beye, M.; Schreck, S.; Grübel, S.; Scholz, M.; Nordlund, D.; Zhang, W.; Hartsock, R. W.; Schlotter, W. F.; Turner, J. J.; Kennedy, B.; Hennies, F.; de Groot, F. M. F.; Gaffney, K. J.; Techert, S.; Odelius, M.; Föhlisch, A. *Nature* **2015**, *520*, 78−81.
(43) Hong, K.; Cho, H.; Schoenlein, R. W.; Kim, T. K.; Huse, N. *Acc. Chem. Res.* **2015**, *48* (11), 2957−2966.
(44) Van Kuiken, B. E.; Cho, H.; Hong, K.; Khalil, M.; Schoenlein, R. W.; Kim, T. K.; Huse, N. *J. Phys. Chem. Lett.* **2016**, *7* (3), 465−470.
(45) Gawelda, W.; Johnson, M.; de Groot, F. M. F.; Abela, R.; Bressler, C.; Chergui, M. *J. Am. Chem. Soc.* **2006**, *128* (15), 5001−5009.
(46) Van Kuiken, B. E.; Huse, N.; Cho, H.; Strader, M. L.; Lynch, M. S.; Schoenlein, R. W.; Khalil, M. *J. Phys. Chem. Lett.* **2012**, *3*, 1695.
(47) Van Kuiken, B. E; Valiev, M.; Daifuku, S. L; Bannan, C.; Strader, M. L; Cho, H.; Huse, N.; Schoenlein, R. W; Govind, N.; Khalil, M. *J. Phys. Chem. A* **2013**, *117*, 4444.
(48) Ross, M.; Van Kuiken, B. E.; Strader, M. L.; Cordones-Hahn, A.; Cho, H.; Schoenlein, R. W.; Kim, T. K.; Khalil, M. *Springer Proc. Phys.* **2015**, *162*, 403−406.
(49) Rittmann-Frank, M. H.; Milne, C. J.; Rittmann, J.; Reinhard, M.; Penfold, T. J.; Chergui, M. *Angew. Chem.* **2014**, *126*, 5968−5972.
(50) Canton, S. E.; Kjær, K. S.; Vankó, G.; van Driel, T. B.; Adachi, S.-i.; Bordage, A.; Bressler, C.; Chabera, P.; Christensen, M.; Dohn, A. O.; Galler, A.; Gawelda, W.; Gosztola, D.; Haldrup, K.; Harlang, T.; Liu, Y.; Møller, K. B.; Németh, Z.; Nozawa, S.; Pápai, M.; Sato, T.; Sato, T.; Suarez-Alcantara, K.; Togashi, T.; Tono, K.; Uhlig, J.; Vithanage, D. A.; Wärnmark, K.; Yabashi, M.; Zhang, J.; Sundström, V.; Nielsen, M. M. *Nat. Commun.* **2015**, *6*, 6359.
(51) Gawelda, W.; Szlachetko, J.; Milne, C. J. *X-Ray Spectroscopy at Free Electron Lasers*; John Wiley & Sons, Ltd., 2016; pp 637−669.
(52) Chergui, M. *Struct. Dyn.* **2016**, *3* (3), 031001.
(53) Shelby, M. L.; Lestrange, P. J.; Jackson, N. E.; Haldrup, K.; Mara, M. W.; Stickrath, A. B.; Zhu, D.; Lemke, H. T.; Chollet, M.; Hoffman, B. M.; Li, X.; Chen, L. X. *J. Am. Chem. Soc.* **2016**, *138* (28), 8752−8764.
(54) Biasin, E.; van Driel, T. B.; Kjær, K. S.; Dohn, A. O.; Christensen, M.; Harlang, T.; Chabera, P.; Liu, Y.; Uhlig, J.; Pápai, M.; Németh, Z.; Hartsock, R.; Liang, W.; Zhang, J.; Alonso-Mori, R.; Chollet, M.; Glownia, J. M.; Nelson, S.; Sokaras, D.; Assefa, T. A.; Britz, A.; Galler, A.; Gawelda, W.; Bressler, C.; Gaffney, K. J.; Lemke, H. T.; Møller, K. B.; Nielsen, M. M.; Sundström, V.; Vankó, G.; Wärnmark, K.; Canton, S. E.; Haldrup, K. *Phys. Rev. Lett.* **2016**, *117*, 013002.
(55) Zhang, W.; Kjaer, K. S.; Alonso-Mori, R.; Bergmann, U.; Chollet, M.; Fredin, L. A.; Hadt, R. G.; Hartsock, R. W.; Harlang, T.; Kroll, T.; Kubicek, K.; Lemke, H. T.; Liang, H. W.; Liu, Y.; Nielsen, M. M.; Persson, P.; Robinson, J. S.; Solomon, E. I.; Sun, Z.; Sokaras, D.; van Driel, T. B.; Weng, T.-C.; Zhu, D.; Warnmark, K.; Sundstrom, V.; Gaffney, K. J. *Chem. Sci.* **2017**, *8*, 515−523.
(56) Haase, J. *J. Phys.: Condens. Matter* **1997**, *9* (18), 3647−3670.
(57) Myneni, S. C. B. *Rev. Mineral. Geochem.* **2000**, *40*, 113−172.
(58) Solomon, E. I.; Hedman, B.; Hodgson, K. O.; Dey, A.; Szilagyi, R. K. *Coord. Chem. Rev.* **2005**, *249* (1−2), 97−129.
(59) Mori, R. A.; Paris, E.; Giuli, G.; Eeckhout, S. G.; Kavcic, M.; Zitnik, M.; Bucar, K.; Pettersson, L. G. M.; Glatzel, P. *Anal. Chem.* **2009**, *81* (15), 6516−6525.
(60) Sproules, S.; Wieghardt, K. *Coord. Chem. Rev.* **2011**, *255* (7−8), 837−860.
(61) Queen, M. S.; Towey, B. D.; Murray, K. A.; Veldkamp, B. S.; Byker, H. J.; Szilagyi, R. K. *Coord. Chem. Rev.* **2013**, *257* (2), 564−578.
(62) Cho, H.; Hong, K.; Strader, M. L.; Lee, J. H.; Schoenlein, R. W.; Huse, N.; Kim, T. K. *Inorg. Chem.* **2016**, *55* (12), 5895−5903.
(63) Khalil, M.; Marcus, M. A.; Smeigh, A. L.; McCusker, J. K.; Chong, H. H. W.; Schoenlein, R. W. *J. Phys. Chem. A* **2006**, *110* (1), 38−44.
(64) Head-Gordon, M.; Pople, J. A.; Frisch, M. J. *Chem. Phys. Lett.* **1988**, *153* (6), 503−506.
(65) Dunning, T. H. *J. Chem. Phys.* **1989**, *90* (2), 1007−1023.
(66) Frisch, M. J.; Trucks, G. W.; Schlegel, H. B.; Scuseria, G. E.; Robb, M. A.; Cheeseman, J. R.; Scalmani, G.; Barone, V.; Mennucci, B.; Petersson, G. A.; Nakatsuji, H.; Caricato, M.; Li, X.; Hratchian, H. P.; Izmaylov, A. F.; Bloino, J.; Zheng, G.; Sonnenberg, J. L.; Hada, M.; Ehara, M.; Toyota, K.; Fukuda, R.; Hasegawa, J.; Ishida, M.; Nakajima, T.; Honda, Y.; Kitao, O.; Nakai, H.; Vreven, T.; Montgomery, J. A., Jr.; Peralta, J. E.; Ogliaro, F.; Bearpark, M.; Heyd, J. J.; Brothers, E.; Kudin, K. N.; Staroverov, V. N.; Kobayashi, R.; Normand, J.; Raghavachari, K.; Rendell, A.; Burant, J. C.; Iyengar, S. S.; Tomasi, J.; Cossi, M.; Rega,

DOI: 10.1021/jacs.6b12992
J. Am. Chem. Soc. 2017, 139, 4797−4804

N.; Millam, J. M.; Klene, M.; Knox, J. E.; Cross, J. B.; Bakken, V.; Adamo, C.; Jaramillo, J.; Gomperts, R.; Stratmann, R. E.; Yazyev, O.; Austin, A. J.; Cammi, R.; Pomelli, C.; Ochterski, J. W.; Martin, R. L.; Morokuma, K.; Zakrzewski, V. G.; Voth, G. A.; Salvador, P.; Dannenberg, J. J.; Dapprich, S.; Daniels, A. D.; Farkas, Ö.; Foresman, J. B.; Ortiz, J. V.; Cioslowski, J.; Fox, D. J., *Gaussian 09 Revision E.01*; Gaussian Inc.: Wallingford CT, 2009.
(67) Andersson, K.; Malmqvist, P. A.; Roos, B. O.; Sadlej, A. J.; Wolinski, K. *J. Phys. Chem.* **1990**, *94* (14), 5483−5488.
(68) Andersson, K.; Malmqvist, P. A.; Roos, B. O. *J. Chem. Phys.* **1992**, *96* (2), 1218−1226.
(69) Malmqvist, P. A.; Pierloot, K.; Shahi, A. R. M.; Cramer, C. J.; Gagliardi, L. *J. Chem. Phys.* **2008**, *128* (20), 204109.
(70) Pinjari, R. V.; Delcey, M. G.; Guo, M.; Odelius, M.; Lundberg, M. *J. Chem. Phys.* **2014**, *141* (12), 124116.
(71) Aquilante, F.; De Vico, L.; Ferre, N.; Ghigo, G.; Malmqvist, P. A.; Neograd y, P.; Pedersen, T. B.; Pitonak, M.; Reiher, M.; Roos, B. O.; Serrano-Andres, L.; Urban, M.; Veryazov, V.; Lindh, R. *J. Comput. Chem.* **2010**, *31* (1), 224−247.
(72) Dewar, P.; Ernstbrunner, E.; Gilmore, J.; Godfrey, M.; Mellor, J. *Tetrahedron* **1974**, *30*, 2455−2459.
(73) Martin, W. C.; Zalubas, R.; Musgrove, A. *J. Phys. Chem. Ref. Data* **1990**, *19* (4), 821−880.
(74) Reva, I.; Nowak, M. J.; Lapinski, L.; Fausto, R. *Phys. Chem. Chem. Phys.* **2015**, *17* (7), 4888−4898.
(75) García-Lastra, J. M.; Cook, P. L.; Himpsel, F. J.; Rubio, A. *J. Chem. Phys.* **2010**, *133*, 151103.
(76) Johnson, P. S.; Cook, P. L.; Zegkinoglou, I.; García-Lastra, J. M.; Rubio, A.; Ruther, R. E.; Hamers, R. J.; Himpsel, F. J. *J. Chem. Phys.* **2013**, *138* (4), 044709.
(77) Castillejo, M.; Couris, S.; Koudoumas, E.; Martín, M. *Chem. Phys. Lett.* **1998**, *289* (3−4), 303−310.

DOI: 10.1021/jacs.6b12992
J. Am. Chem. Soc. 2017, 139, 4797−4804